

## Local lattice distortion of Ge-dilute Ge-Si alloy: Multiple-scattering EXAFS study

Zhihu Sun,<sup>1</sup> Wensheng Yan,<sup>1</sup> Hiroyuki Oyanagi,<sup>2</sup> Zhiyu Pan,<sup>1</sup> and Shiqiang Wei<sup>1,\*</sup>

<sup>1</sup>National Synchrotron Radiation Laboratory, University of Science and Technology of China, Hefei, Anhui 230029, People's Republic of China

<sup>2</sup>Photonic Institute, National Institute of Advanced Industrial Science and Technology, 1-1-4 Umezono, Tsukuba, Ibaraki 305-8568, Japan  
(Received 5 April 2006; revised manuscript received 18 June 2006; published 21 September 2006)

The local structure of a  $\text{Ge}_{0.006}\text{Si}_{0.994}$  thin film with dilute Ge impurity in a Si host has been studied by fluorescence x-ray absorption fine structure spectroscopy in the temperature region of 10–300 K using the multiple-scattering data analysis method. Contrary to the elongation of 0.029 Å for the Ge-Si distance in the first shell, the Ge-Si interatomic distance in the second shell shows a contraction of about 0.013 Å relative to the corresponding Si-Si distance in the Si host. This coincides with the theoretical result calculated using the formula proposed by Mousseau and Thorpe [Phys. Rev. B **46**, 15887 (1992)] which includes both the bond-length mismatch and bond-angle deviation. It turns out that the contraction of the second-shell Ge-Si distance is due to the deviation of the Ge-Si-Si bond angle from the ideal tetrahedral angle. From the obtained Ge-Si distances within the first three shells, it is revealed that dilute Ge doped into a Si host can lead to local distortion rather than an average lattice change.

DOI: 10.1103/PhysRevB.74.092101

PACS number(s): 61.10.Ht, 61.72.Tt, 68.55.Ln

In the last decade, crystalline Ge-Si alloys and heterostructures have attracted much attention, due to their significantly improved electronic properties with relatively simple incorporation into existing Si technology.<sup>1</sup> The 4.2% mismatch for the lattice constants between Ge and Si crystals leads to significant strain during the epitaxial growth of Ge-Si thin films, and consequently modifies the band structure. It has long been known that the nonlinear variation of the band gap of  $\text{Ge}_x\text{Si}_{1-x}$  alloys with composition is associated with the displacement of the microscopic atomic structure from the ideal lattice sites<sup>2</sup> which were often assumed in terms of the virtual crystal approximation.<sup>3</sup> Therefore understanding the local structure of  $\text{Ge}_x\text{Si}_{1-x}$  alloys is essential to precisely calculate their band structures. For this purpose, a lot of experimental<sup>4</sup> and theoretical<sup>5–10</sup> work has been done to investigate the composition dependence of the bond lengths; unfortunately, some discrepancy still exists.

Most of the experimental investigations on  $\text{Ge}_x\text{Si}_{1-x}$  alloys by using extended x-ray absorption fine structure (EXAFS) spectroscopy mainly focus on the variation of Ge-Si and Ge-Ge bond lengths with  $x$ . Few results regarding  $\text{Ge}_x\text{Si}_{1-x}$  alloys in the dilute limit ( $x \sim 0$ ) can be found in the literature.  $\text{Ge}_x\text{Si}_{1-x}$  alloys of dilute Ge content can provide a good opportunity to investigate the lattice distortion around Ge atoms in the Si host and to test the validity of theoretical calculations in the limiting cases. It is also expected that Ge-dilute Ge-Si alloys are favorable to address the effects of Coulomb forces.<sup>11</sup> Experimentally, structural information in Ge-dilute alloys can be more accurately determined by EXAFS than in  $\text{Ge}_x\text{Si}_{1-x}$  alloys with higher Ge content, since in the former Ge atoms are solely coordinated by Si atoms while in the latter EXAFS contributions of Ge-Si and Ge-Ge pairs are overlapped.

Recently, Pascarella *et al.*,<sup>12</sup> Tormen *et al.*,<sup>13</sup> and we<sup>14,15</sup> have used the multiple-scattering (MS) EXAFS method to study the high-shell local structures for III-V and IV-IV semiconductors with diamond and zinc-blende structures. For pseudobinary strained alloys it was shown that structural modifications due to tetragonal distortion appear mainly in

the second and third shells<sup>12,13</sup> and that the strain due to alloying is released mainly through bond-angle distortions.<sup>16</sup> However, for Ge-Si alloys experimental EXAFS results regarding the higher shells can hardly be found. Due to the similarity between the structures of III-V semiconductors and Ge-Si alloys, it can be expected that the tetrahedral building block in Ge-Si alloys is also distorted so as to accommodate simultaneously a bimodal distribution of bond lengths and long-range order. In order to well determine the distortion of the unit cell in Ge-Si alloys, it is of importance to extend the local structure study for Ge-Si alloys to higher shells. The structural information of high shells is useful to address both bond-length and bond-angle accommodation of strain.<sup>15,17</sup>

In this paper, a MS EXAFS analysis is performed to study the local structures around Ge atoms up to the third shell for the  $\text{Ge}_x\text{Si}_{1-x}$  alloy in the dilute Ge limit ( $x=0.006$ ). We aim to investigate the local lattice distortion including both bond-length and bond-angle variations induced by the dilute Ge impurity.

The  $\text{Ge}_{0.006}\text{Si}_{0.994}$  thin film sample was prepared by molecular beam epitaxy (MBE), which was described elsewhere.<sup>18</sup> Boron-doped Si (001) substrate (10 Ω cm) was chemically cleaned by the Shiraki method prior to insertion into the vacuum. The 2-μm-thick heteroepitaxial  $\text{Ge}_{0.006}\text{Si}_{0.994}$  thin film was deposited on a substrate of Si (001) at 673 K in a MBE growth chamber with a base pressure of  $1 \times 10^{-10}$  Torr.

XAFS measurements were performed at BL-13B of the Photon Factory of the National Laboratory for High Energy Physics (KEK). The electron beam energy was 2.5 GeV and the maximum stored current was 400 mA. A hard x-ray coming from a 27-pole wiggler with a maximum magnetic field of 1.5 T inserted in the straight section of the storage was used. The Ge *K*-edge XAFS spectra of the  $\text{Ge}_{0.006}\text{Si}_{0.994}$  thin film were recorded in fluorescence mode by using a 19-element pure Ge solid-state detector. Three independent XAFS measurements were carried out at different temperatures of 20, 100, and 300 K, especially at low temperatures

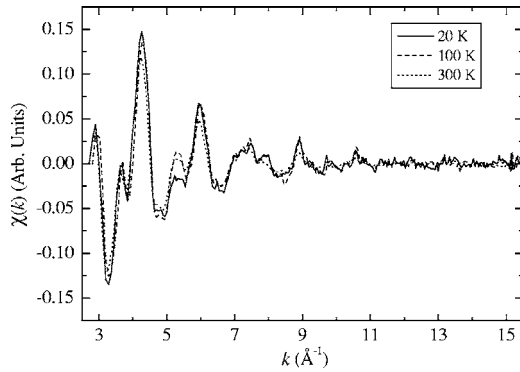


FIG. 1. Ge  $K$ -edge EXAFS oscillation function  $\chi(k)$  for  $\text{Ge}_{0.006}\text{Si}_{0.994}$  thin film recorded at 20, 100, and 300 K.

to minimize thermal disorder. The detailed experiment procedure can be found elsewhere.<sup>19</sup> EXAFS data were analyzed by using the USTC-XAFS3.0 software package<sup>20</sup> compiled by Zhong and Wei according to standard procedures.

Figure 1 shows the Ge  $K$ -edge EXAFS function  $\chi(k)$  of the  $\text{Ge}_{0.006}\text{Si}_{0.994}$  thin film measured at temperatures of 20, 100, and 300 K. All the  $\chi(k)$  functions exhibit strong oscillations in the low- $k$  region with the maximum at about  $k = 4 \text{ \AA}^{-1}$ , then decrease sharply with increase of  $k$ . This characteristic indicates that the Ge atoms in the  $\text{Ge}_{0.006}\text{Si}_{0.994}$  thin film are predominantly surrounded by the light element Si. The solid lines in Fig. 2 show the radial structural functions of the  $\text{Ge}_{0.006}\text{Si}_{0.994}$  thin film obtained from Fourier transforming their  $k^2\chi(k)$  spectra. Three peaks located at about 2.0, 3.4, and 4.1  $\text{\AA}$  are related to the first, second, and third coordination shells around Ge atoms, respectively. The strong high-shell peaks allow us to perform a MS analysis on the local structure beyond the first shell around Ge atoms.

For quantitative analysis, a least-squares curve fit including the MS contributions was performed by using the FEFFIT code of the UWXAFS3.0 package.<sup>21</sup> The theoretical scattering amplitude and phase-shift functions of all the single-scattering (SS) and MS paths in the first three shells were calculated by FEFF7.<sup>22</sup> The starting model structure for the FEFF7 calculation is a Ge atom replacing the site of the central Si atom in a Si cluster, and keeping the position of all Si neighbors unchanged. From our previous results on the MS effects in diamond and zinc-blende structures,<sup>14,15</sup> for analyzing the local structures in the first three shells it is enough to consider three single-scattering paths plus one dominant triangular double-scattering path  $\text{Ge} \rightarrow \text{Si}_1 \rightarrow \text{Si}_2 \rightarrow \text{Ge}$ , which interferes destructively with the SS path of the second coordination shell.

The fits to the EXAFS spectra of  $\text{Ge}_{0.006}\text{Si}_{0.994}$  thin film were done in  $R$  space. In the fitting procedure the coordination number was fixed to the nominal value for each scattering path, and the amplitude reduction factor  $S_0^2$  was also fixed to be the best-fit value 0.87 in crystalline Ge.<sup>15</sup> Special care was taken to extract the high-shell structural information with high accuracy. We analyzed the data in two steps. First, a single-shell fit for the nearest Ge-Si coordination was done in the  $R$  range  $[1.2, 2.5] \text{ \AA}$  by varying these parameters: bond length  $R_1$ , Debye-Waller factor  $\sigma_1^2$ , and shift of the energy origin  $\Delta E_0$ . Second, in the MS fits for higher shells in the  $R$

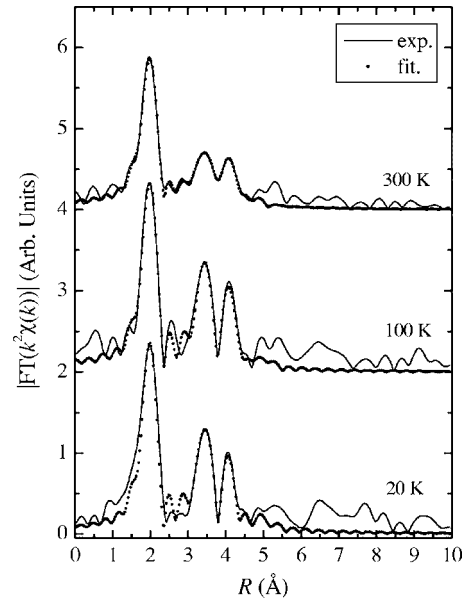


FIG. 2. Radial structural function obtained by Fourier transforming  $k^2\chi(k)$  for  $\text{Ge}_{0.006}\text{Si}_{0.994}$  thin film recorded at 20, 100, and 300 K: experimental (solid line) and fitting (circles).

range  $[2.5, 4.8] \text{ \AA}$ ,  $\sigma^2$  and  $R$  for each path were treated as adjustable parameters, while  $\Delta E_0$  was fixed to the best-fit value for the first shell. In this way the correlation between  $R$  and  $\Delta E_0$  was reduced. This approximation is reasonable, since Ge and Si are isovalent atoms and have very close values of electronegativity. Therefore the electrostatic potentials induced by charge transfer between Ge and Si atoms can be neglected, and the approximation of neutral absorber atom assumed by FEFF7 is valid, so that an overall  $\Delta E_0$  is enough for all scattering events. The overall fitting results are shown in Fig. 2 as dotted lines, and the best-fit structural parameters are summarized in Table I. The determination of error bars is consistent with the criteria adopted by the International XAFS Society,<sup>23</sup> i.e., estimated from the square root of the diagonal elements of the correlation matrix.

It should be noted that the directly extracted Ge-Si interatomic distances at different temperatures should be slightly temperature dependent due to the effect of thermal expansion. In order to compare these results on the same basis, the distances at lower temperatures are corrected to the values at room temperature by approximating the thermal expansion coefficient of Ge-Si bonds to be the averaged value for Ge and Si crystals, namely,  $4.3 \times 10^{-6} \text{ K}^{-1}$ . This causes a contraction of the nearest Ge-Si bond length by 0.003  $\text{\AA}$  (0.002  $\text{\AA}$ ) at 20 K (100 K) relative to that at 300 K. The corrected  $R_{\text{Ge-Si}}$  values, denoted as  $R^{rt}$ , are included in the last column of Table I.

After correcting the thermal expansion effect, Table I indicates that the averaged Ge-Si bond length of the first shell is 2.381  $\text{\AA}$  at 300 K, larger than the Si-Si bond length 2.352  $\text{\AA}$  in crystalline Si by 0.029  $\text{\AA}$ . The difference in atomic size between Ge and Si causes a local compressive strain in the first nearest neighbor around Ge atoms. Therefore, in order to compensate for the bond-length mismatch, the nearest Si atoms are displaced away from Ge impurity atoms toward the  $[111]$  direction, as shown schematically in Fig. 3.

TABLE I. The structural parameters of crystalline Si, Ge, and  $\text{Ge}_{0.006}\text{Si}_{0.994}$  samples at different temperatures. The underlined values are fixed in the fits.  $R^r$  in the last column is the interatomic distance at room temperature after correcting for the thermal expansion effect.

Sample	Shell	$R$ (Å)	$\sigma^2$ ( $10^{-3}$ Å <sup>2</sup> )	$\Delta E_0$ (eV)	$R^r$ (Å)
$\text{Ge}_{0.006}\text{Si}_{0.994}$ (20 K)	1	$2.378 \pm 0.008$	$1.8 \pm 0.9$	$8.7 \pm 1.0$	2.381
	2	$3.823 \pm 0.012$	$3.7 \pm 1.5$	<u>8.7</u>	3.828
	3	$4.489 \pm 0.030$	$4.6 \pm 4.3$	<u>8.7</u>	4.495
$\text{Ge}_{0.006}\text{Si}_{0.994}$ (100 K)	1	$2.376 \pm 0.008$	$2.0 \pm 0.6$	$8.7 \pm 1.0$	2.378
	2	$3.828 \pm 0.012$	$4.0 \pm 1.0$	<u>8.7</u>	3.831
	3	$4.486 \pm 0.030$	$4.9 \pm 1.8$	<u>8.7</u>	4.490
$\text{Ge}_{0.006}\text{Si}_{0.994}$ (300 K)	1	$2.384 \pm 0.008$	$4.0 \pm 0.5$	$8.4 \pm 0.8$	2.384
	2	$3.835 \pm 0.012$	$9.6 \pm 1.1$	<u>8.4</u>	3.835
	3	$4.490 \pm 0.030$	$10.8 \pm 1.7$	<u>8.4</u>	4.490
Crystalline Si	1	2.352			
	2	3.841			
	3	4.504			
Crystalline Ge	1	2.453			
	2	4.005			
	3	4.696			

Contrary to the elongated Ge-Si bond in the first shell, a more intriguing result can be found from Table I: the Ge-Si interatomic distance in the second shell for the  $\text{Ge}_{0.006}\text{Si}_{0.994}$  alloy is slightly contracted relative to the corresponding Si-Si distance 3.841 Å. At first glance it may be doubtful whether this contraction arises from the random error of a single XAFS measurement. To check the repeatability of this result we measured the XAFS spectra at different temperatures, especially at low temperatures. Three independent measurements yield the room-temperature Ge-Si distances in the second shell to be 3.828, 3.831, and 3.835 Å, respectively. All of them are uniformly shorter than 3.841 Å. The accuracy in determination of the Ge-Si distance is 0.012 Å, better than the commonly accepted EXAFS accuracy of 0.02 Å, due to the high signal-to-noise ratio of the EXAFS spectra and the refined data analysis procedure we have used. In fact, the

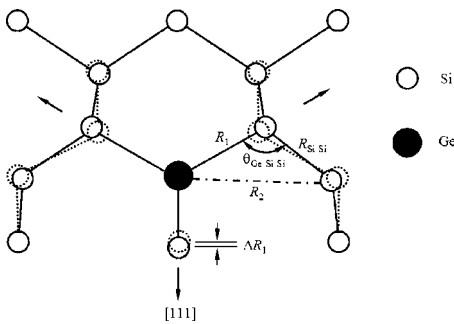


FIG. 3. Schematic diagram of the local structure of a dilute Ge impurity in the Si host matrix. The black circle represents a Ge atom and the white circles represent Si atoms. The white circles with dotted borders represent the locations in the diamond structure.

highest accuracy reported in the distance determination by EXAFS can be as high as 0.002 Å for the first shell,<sup>24,25</sup> and 0.006 Å for higher shells.<sup>12,13</sup>

The contraction of the second-nearest Ge-Si distance seems a little surprising, but coincides with a previous theoretical estimate by Mousseau and Thorpe,<sup>6</sup> who calculated the second-nearest distance  $R_2^{\text{GeSiSi}}$  in  $\text{Ge}_x\text{Si}_{1-x}$  alloy by taking into account both the bond-length mismatch and angular deviation,

$$R_2^{\text{GeSiSi}} = \sqrt{\frac{8}{3}} [(1-x)R_0^{\text{Si-Si}} + xR_0^{\text{Ge-Ge}}] \times e^{-(1/8)(\Delta\theta)^2} \frac{\sin(\langle\theta_{\text{Ge-Si-Si}}\rangle/2)}{\sin(\theta_0/2)} - \frac{1}{2} a^{**} (R_0^{\text{Ge-Ge}} - R_0^{\text{Si-Si}}) \times \left[ \sqrt{\frac{8}{3}} x + \sqrt{\frac{3}{8}} \left( x - \frac{1}{2} \right) \right]. \quad (1)$$

Here  $R_0^{\text{Si-Si}}$  and  $R_0^{\text{Ge-Ge}}$  are the nearest Si-Si and Ge-Ge bond lengths in crystalline Si and Ge,  $\langle\theta_{\text{Ge-Si-Si}}\rangle$  is the averaged Ge-Si-Si bond angle,  $\langle\Delta\theta\rangle$  is its standard deviation,  $\theta_0 = 109.47^\circ$ , and  $a^{**} \approx 0.7$  is the topological rigidity parameter.

In the case of the  $\text{Ge}_{0.006}\text{Si}_{0.994}$  alloy,  $x = 0.006$ , the second term on the right hand side of Eq. (1) is equal to 0.010 Å. This increased second-nearest Ge-Si-Si distance is ascribed to the topological rigidity of the lattice. Then

$$R_2^{\text{GeSiSi}} = 3.842 e^{-(1/8)(\Delta\theta)^2} \frac{\sin(\langle\theta_{\text{Ge-Si-Si}}\rangle/2)}{\sin(\theta_0/2)} + 0.010 \text{ Å}. \quad (2)$$

Before obtaining the quantitative result for  $R_2^{\text{GeSiSi}}$ , it is necessary to know the averaged Ge-Si-Si bond angle  $\langle\theta_{\text{Ge-Si-Si}}\rangle$  and its standard deviation  $\langle\Delta\theta\rangle$ .

$\langle\Delta\theta\rangle$  can be evaluated through the total standard deviation  $\langle\Delta\theta\rangle_{\text{total}}$  of the Ge-Si-Si bond angle. Using standard differential techniques as suggested by Baker *et al.*,<sup>26</sup>  $\langle\Delta\theta\rangle_{\text{total}}$  can be calculated from the Debye-Waller factors  $\sigma_1^2$  and  $\sigma_2^2$  of the first and second Ge-Si pairs and  $\sigma_{\text{Si-Si}}^2$  of the nearest Si-Si bond,

$$\langle\Delta\theta\rangle_{\text{total}}^2 = \frac{1}{4R_1^2 R_{\text{Si-Si}}^2 - (R_1^2 + R_{\text{Si-Si}}^2 - R_2^2)^2} \times \left( \frac{(R_1^2 - R_{\text{Si-Si}}^2 + R_2^2)^2}{R_1^2} \sigma_1^2 + 4R_2^2 \sigma_2^2 + \frac{(R_{\text{Si-Si}}^2 - R_1^2 + R_2^2)^2}{R_1^2} \sigma_{\text{Si-Si}}^2 \right). \quad (3)$$

Our EXAFS results in Table I include only the Debye-Waller factors of the Ge-Si pairs, but not that of the Si-Si bond. Fortunately, the temperature dependence of the Debye-Waller factors of the Si-Si bond has been theoretically calculated by Benfatto *et al.*<sup>27</sup> who obtained  $\sigma_{\text{Si-Si}}^2(20 \text{ K}) \approx \sigma_{\text{Si-Si}}^2(100 \text{ K}) = 0.0026 \text{ Å}^2$  and  $\sigma_{\text{Si-Si}}^2(300 \text{ K}) = 0.0034 \text{ Å}^2$ . From Eq. (3), we can estimate  $\langle\Delta\theta\rangle_{\text{total}}$  to be  $\pm 3.4^\circ$ ,  $\pm 3.5^\circ$ ,

and  $\pm 5.0^\circ$  for the  $\text{Ge}_{0.006}\text{Si}_{0.994}$  thin film at the temperatures of 20, 100, and 300 K, respectively. The value of  $\langle \Delta\theta \rangle_{\text{total}}$  for the  $\text{Ge}_{0.006}\text{Si}_{0.994}$  thin film at 300 K is identical with that ( $\pm 5^\circ$ ) in crystalline GaAs,<sup>26</sup> indicating that the bond-angle standard deviation in the  $\text{Ge}_{0.006}\text{Si}_{0.994}$  thin film is rather small.

It should be kept in mind that  $\langle \Delta\theta \rangle_{\text{total}}$  consists of configurational and thermal disorder as the bond-length disorder does. The  $\langle \Delta\theta \rangle$  in Eq. (2) is only the configurational part, and should be temperature independent. Even at the lowest temperature of 20 K,  $\langle \Delta\theta \rangle$  is still smaller than  $\langle \Delta\theta \rangle_{\text{total}} = 3.4^\circ$ ; therefore  $e^{-(1/8)(\langle \Delta\theta \rangle^2)} > e^{-(1/8)(3.4\pi/180)^2} = 0.9996$ . This means that for the  $\text{Ge}_{0.006}\text{Si}_{0.994}$  thin film the second-nearest Ge-Si distance contraction due to the bond-angle standard deviation is less than 0.04% and can be safely neglected. Equation (2) is further simplified to be

$$R_2^{\text{GeSiSi}} = 3.842 \frac{\sin(\langle \theta_{\text{Ge-Si-Si}} \rangle / 2)}{\sin(\theta_0 / 2)} + 0.010 \text{ \AA}. \quad (4)$$

From Eq. (4) the contraction of the second-shell Ge-Si distance is indeed possible, provided that  $\langle \theta_{\text{Ge-Si-Si}} \rangle$  is obviously smaller than  $\theta_0 = 109.47^\circ$ . The bond angle  $\langle \theta_{\text{Ge-Si-Si}} \rangle$  in crystalline  $\text{Ge}_x\text{Si}_{1-x}$  alloys has been theoretically calculated by Yu *et al.* using an *ab initio* molecular dynamics scheme<sup>7</sup> and by Tzoumanekas *et al.* using Monte Carlo simulations.<sup>9</sup> Both calculations give very close values of  $\langle \theta_{\text{Ge-Si-Si}} \rangle = 108.7^\circ$  in the  $x \sim 0$  limit. Substituting this result into Eq. (4)

we get  $R_2^{\text{GeSiSi}} = 3.834 \text{ \AA}$ , which is shorter than the expected value  $3.841 \text{ \AA}$  and is very close to our averaged experimental result  $3.831 \text{ \AA}$ . Figure 3 schematically shows the effect of Ge-Si-Si bond-angle deviation on the second-shell Ge-Si distance. It is this slight deviation of the Ge-Si-Si bond angle that leads to the contraction of the second-shell Ge-Si distance which compensates for the increased distance due to topological rigidity. Summarizing the experimental and theoretical results, we believe that in  $\text{Ge}_x\text{Si}_{1-x}$  ( $x \sim 0$ ) alloys the second-nearest Ge-Si distance is shorter than the corresponding Si-Si distance.

It also needs to be pointed out that the distance change of the second and third shells with regard to the corresponding Si-Si distance is only at the level of  $0.01 \text{ \AA}$ , obviously less than the change of  $0.029 \text{ \AA}$  in the first shell. This indicates that the position displacement of Si neighbors around Ge atoms is much more significant in the first shell than in the higher shells upon doping of a Ge impurity into a Si host. This behavior can be easily understood by taking into account the loosely packed atoms in the diamond structure. Therefore, the local distortion around the Ge impurity in the  $\text{Ge}_{0.006}\text{Si}_{0.994}$  thin film is prominently limited to the first nearest neighbors and the mismatch strain is nearly relieved in more distant atoms. Doping Ge into Si host introduces local distortion rather than an average lattice change.

This work was supported by the National Science Foundation of China (Grants No. 10375059 and No. 10404023) and the Cooperation Program between BSRF and NSRL.

\*Corresponding author. Electronic address: sqwei@ustc.edu.cn

- <sup>1</sup>U. Konig and H. Dambkes, *Solid-State Electron.* **38**, 1595 (1995).
- <sup>2</sup>A. Zunger and J. E. Jaffe, *Phys. Rev. Lett.* **51**, 662 (1983).
- <sup>3</sup>R. Bisaro, P. Merenda, and T. P. Pearsall, *Appl. Phys. Lett.* **34**, 4457 (1979).
- <sup>4</sup>See, for example, C. Lamberti, *Surf. Sci. Rep.* **53**, 1 (2004), and references therein.
- <sup>5</sup>J. L. Martins and A. Zunger, *Phys. Rev. B* **30**, 6217 (1984).
- <sup>6</sup>N. Mousseau and M. F. Thorpe, *Phys. Rev. B* **46**, 15887 (1992).
- <sup>7</sup>M. Yu, C. S. Jayanthi, D. A. Drabold, and S. Y. Wu, *Phys. Rev. B* **64**, 165205 (2001).
- <sup>8</sup>P. Venezuela, G. M. Dalpian, Antonio J. R. da Silva, and A. Fazzio, *Phys. Rev. B* **64**, 193202 (2001).
- <sup>9</sup>C. Tzoumanekas and P. C. Kelires, *Phys. Rev. B* **66**, 195209 (2002).
- <sup>10</sup>M. Ishimaru, M. Yamaguchi, and Y. Hirotsu, *Phys. Rev. B* **68**, 235207 (2003).
- <sup>11</sup>J. C. Woicik, K. E. Miyano, C. W. King, R. W. Johnson, J. G. Pellegrino, T. L. Lee, and Z. H. Lu, *Phys. Rev. B* **57**, 14592 (1998).
- <sup>12</sup>S. Pascarelli, F. Boscherini, C. Lamberti, and S. Mobilio, *Phys. Rev. B* **56**, 1936 (1997).
- <sup>13</sup>M. Tormen, D. De Salvador, A. V. Drigo, F. Romanato, F. Boscherini, and S. Mobilio, *Phys. Rev. B* **63**, 115326 (2001).
- <sup>14</sup>S. Q. Wei and Z. H. Sun, *J. Phys.: Condens. Matter* **17**, 8017 (2005).
- <sup>15</sup>Z. H. Sun, S. Q. Wei, A. V. Kolobov, H. Oyanagi, and K. Brun-

ner, *Phys. Rev. B* **71**, 245334 (2005).

- <sup>16</sup>J. C. Woicik, J. G. Pellegrino, B. Steiner, K. E. Miyano, S. G. Bompadre, L. B. Sorensen, T. L. Lee, and S. Khalid, *Phys. Rev. Lett.* **79**, 5026 (1997).
- <sup>17</sup>J. C. Aubry, T. Tyliczszak, A. P. Hitchcock, J. M. Bavibeau, and T. E. Jackman, *Phys. Rev. B* **59**, 12872 (1999).
- <sup>18</sup>S. Q. Wei, H. Oyanagi, H. Kawanami, K. Sakamoto, T. Sakamoto, K. Tamura, N. L. Saini, and K. Uosaki, *J. Appl. Phys.* **82**, 4810 (1997).
- <sup>19</sup>H. Oyanagi, M. Martini, and M. Saito, *Nucl. Instrum. Methods Phys. Res. A* **403**, 58 (1998).
- <sup>20</sup>W. Zhong and S. Wei, *J. Chin. Univ. Sci. Technol.* **31**, 328 (2001).
- <sup>21</sup>E. A. Stern, M. Newville, B. Ravel, Y. Yakoby, and D. Haskel, *Physica B* **208**, 117 (1995).
- <sup>22</sup>J. Mustre de Leon, J. J. Rehr, S. I. Zabinsky, and R. C. Albers, *Phys. Rev. B* **44**, 4146 (1991).
- <sup>23</sup>F. W. Lytle, D. E. Sayers, and E. A. Stern, *Physica B* **158**, 701 (1989).
- <sup>24</sup>Y. Kuwahara, H. Oyanagi, R. Shioda, Y. Takeda, H. Kamei, and M. Aono, *J. Appl. Phys.* **82**, 214 (1997).
- <sup>25</sup>R. Shioda, H. Oyanagi, Y. Kuwahara, Y. Takeda, K. Haga, and H. Kamei, *Jpn. J. Appl. Phys., Part 1* **33**, 5623 (1994).
- <sup>26</sup>S. H. Baker, S. C. Bayliss, S. J. Gurman, N. Elgun, J. S. Bates, and E. A. Davis, *J. Phys.: Condens. Matter* **5**, 519 (1993).
- <sup>27</sup>M. Benfatto, C. R. Natoli, and A. Filipponi, *Phys. Rev. B* **40**, 9626 (1989).